How to cite: *Angew. Chem. Int. Ed.* **2022,** *61,* e202211066
International Edition: doi.org/10.1002/anie.202211066
German Edition: doi.org/10.1002/ange.202211066

Physical Chemistry | Hot Paper

From Local Covalent Bonding to Extended Electric Field Interactions in Proton Hydration

Maria Ekimova, Carlo Kleine, Jan Ludwig, Miguel Ochmann, Thomas E. G. Agrenius, Eve Kozari, Dina Pines, Ehud Pines, Nils Huse, Philippe Wernet,* Michael Odelius,* and Erik T. J. Nibbering**

Abstract: Seemingly simple yet surprisingly difficult to probe, excess protons in water constitute complex quantum objects with strong interactions with the extended and dynamically changing hydrogen-bonding network of the liquid. Proton hydration plays pivotal roles in energy transport in hydrogen fuel cells and signal transduction in transmembrane proteins. While geometries and stoichiometry have been widely addressed in both experiment and theory, the electronic structure of these specific hydrated proton complexes has remained elusive. Here we show, layer by layer, how utilizing novel flatjet technology for accurate x-ray spectroscopic measurements and combining infrared spectral analysis and calculations, we find orbital-specific markers that distinguish two main electronic-structure effects: Local orbital interactions determine covalent bonding between the proton and neigbouring water molecules, while orbital-energy shifts measure the strength of the extended electric field of the proton.

[*] Dr. M. Ekimova, C. Kleine, J. Ludwig, Dr. E. T. J. Nibbering
Max Born Institut für Nichtlineare Optik und Kurzzeitspektroskopie
Max Born Strasse 2A, 12489 Berlin (Germany)
E-mail: nibberin@mbi-berlin.de

Dr. M. Ochmann, Prof. Dr. N. Huse
Institute for Nanostructure and Solid State Physics, Center for Free-Electron Laser Science
Luruper Chaussee 149, 22761 Hamburg (Germany)

T. E. G. Agrenius, Prof. Dr. M. Odelius
Department of Physics, Stockholm University
AlbaNova University Center
106 91 Stockholm (Sweden)
E-mail: odelius@fysik.su.se

Dr. E. Kozari, Dr. D. Pines, Prof. Dr. E. Pines
Department of Chemistry, Ben Gurion University of the Negev
P.O.B. 653, Beersheva 84105 (Israel)
E-mail: epines@bgu.ac.il

Prof. Dr. P. Wernet
Department of Physics and Astronomy, Uppsala University
Box 516 Lägerhyddsvägen 1, 751 20 Uppsala (Sweden)
E-mail: philippe.wernet@physics.uu.se

Introduction

Aqueous proton transport, ubiquitous in chemistry and biology, involves decisive roles of individual water molecules, as demonstrated for cases as diverse as the von Grotthuss mechanism,[1] acid-base neutralization reactions,[2] proton transport in hydrogen fuel cells,[3] and transmembrane proteins controlling the proton gradient along biological membranes.[4] Numerous experimental[5] and theoretical studies[1,6a,b–e] have provided compelling evidence for structurally well-defined hydrated proton complexes with specific stoichiometries that are understood to occur at distinct stages of proton transport.

Conceptually, the most simple and smallest configuration of an aqueous proton is the hydronium ion, H_3O^+, with its tripyramidal arrangement of the O–H bonds and an electron-deficient lone pair. H_3O^+ is the central unit in an Eigen cation, $H_3O^+(H_2O)_3$,[7] with the O–H groups forming medium-strong hydrogen bonds to three nearest water molecules, with average heavy atom O···O distances of 2.5–2.6 Å.[8] Alternatively, a proton can be shared between two water molecules in a Zundel cation, $H_5O_2^+$.[9] For this configuration, a superstrong hydrogen bond has been reported (with an O···H^+···O distance of 2.4 Å[8,10]), with weaker hydrogen bonds to its first solvation shell (O···O distances of ≈2.7 Å, closer to the O···O distance of 2.8 Å in bulk liquid water). While hydrogen bond length distributions and the impact of solvent shell fluctuations on ultrafast time scales have now been well reported,[5d,f,h,i,11] little is known about the electronic structure of the hydrated proton in solution as suitable experimental probes have only recently become available. Soft x-ray absorption spectroscopy (XAS) is a powerful tool[12] to monitor electronic structure from a local atomic perspective and on an orbital level via excitations of the 1s core electrons to the lowest unoccupied molecular orbitals (LUMOs). Whereas the highest occupied molecular orbitals (HOMOs) are obviously responsible for chemical bonding as described by wavefunction based occupied molecular orbitals, LUMOs are not just the anti-bonding partner of its respective HOMOs, but in addition LUMOs are more polarizable and so more sensitive to changes in bonding caused by nearest neighbour interactions. For instance, the impact of hydrogen bonding on the electronic structure has been extensively studied using XAS at the oxygen K-edge for water,[13] alcohols and solutes.[14] Here we report on our XAS measurements on

hydrated proton complexes in acetonitrile solution. We show that with this approach we can fully grasp the O K-edge absorption spectra of these hydrated proton complexes without major solvent contributions, whereas for oxygen containing solvents essential spectral ranges would be opaque and so become inaccessible. We provide with supporting FT-IR measurements evidence for practically all water molecules participating in proton hydration with the average size of the hydrated proton complex determined by the molar ratio between acid and water. A detailed characterization of the possible stoichiometries (chemical speciation) when using strong mineral acids in acetonitrile solution is provided, and together with ab initio molecular dynamics (AIMD) simulations we show which possible structural hierarchies in the hydrated proton complexes occur. Quantum chemical calculations of the XAS contributions of the individual water molecules in these hydrated proton complexes then will elucidate to what extent the electronic structure of the contributing water molecules are modified when hydrating the excess proton, and to which spatial range the positive charge of the proton can play a significant role in modifying the O K.edge XAS of water as compared with those of unprotonated water.

Results and Discussion

In Figure 1 we compare the O K-edge absorption spectra of H_2O in the gas phase, of the H_2O monomer in acetonitrile solution and of the mineral acid/water/acetonitrile solution for which 86% of the water molecules are part of $H_7O_3^+$ hydrated proton complexes. For details on these measurements we refer to the Methods section and Supporting Information Figures S1 and S2 in Supporting Information Section 1. Details on how to disentangle in these measurements possible contributions of additional water molecules in larger hydrated proton complexes are discussed in the Supporting Information Section 2 (see also Figure S3). For this we make use of our findings on the clear distinctive hierarchy of hydrogen bonding interactions of hydrated proton complexes of particular sizes. This hydrogen bond hierarchy enables us to discuss proton hydration in terms of associated structural motifs, and in a distinction between

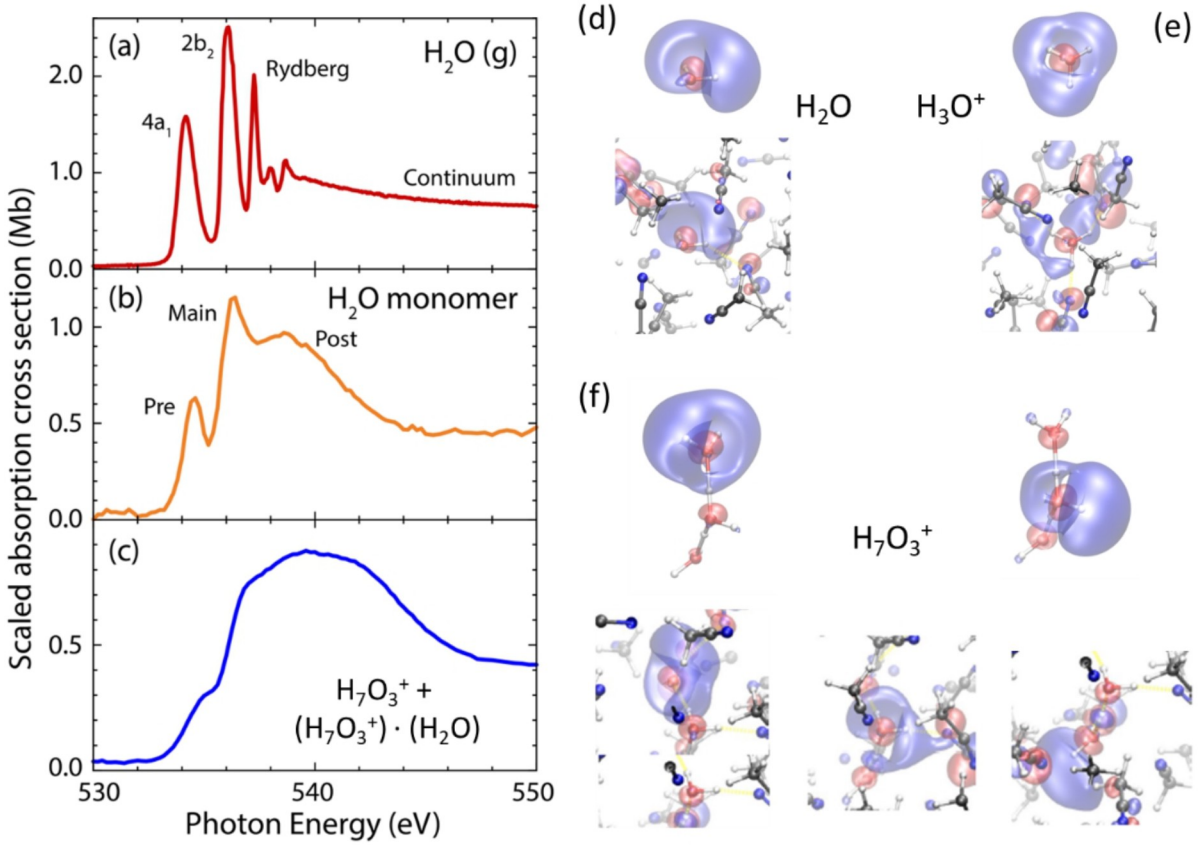

Figure 1. O K-edge absorption spectra of a) H_2O in the gas phase, b) H_2O monomer in acetonitrile solution, and c) the hydrated proton complex $H_7O_3^+$ prepared in acetonitrile prepared as 50% $H_7O_3^+$ and 50% $H_7O_3^+ \cdot H_2O$, i.e. the $H_7O_3^+$ moiety, equivalent to a [w1·H_3O^+·w2] complex, contributes about 86% to the experimental O K-edge spectrum, and w3 only with 14%. The gas phase result of H_2O was taken from ref. [13b]. Snapshots of the $4a_1$ LUMO, contributing to the pre-edge peak, for the water monomer (d) and H_3O^+ (e), both as isolated species and as solute embedded in acetonitrile solution. The similar shapes of the LUMOs of $H_7O_3^+$, reached upon oxygen 1s core excitation from the respective H_2O and H_3O^+ units, are also clearly apparent (f).

proximal and distal water molecules in the hydrated proton complexes (vide infra). Figure 1 provides a direct indication for how different the electronic structure is in the three systems. The H_2O monomer spectrum was measured with a solution of 0.75 mM of H_2O in acetonitrile. Instead of using aqueous acid solutions,[15] we prepared the hydrated proton complexes in acetonitrile. Strong mineral acids are able to protonate water in acetonitrile, forming hydrated proton complexes with an average complex size depending on the acid-to-water ratio. For (sub)molar concentrations of acid and water, practically all water molecules are involved in proton hydration, as previous IR-spectroscopy studies[5b,f,11,5i] and our own IR measurements show (see Supporting Information).

The spectrum of the isolated H_2O molecule (Figure 1a) is dominated by the two main peaks due to 1s to LUMO ($4a_1$) and LUMO+1 ($2b_2$) single electron transitions.[13b,16] For the H_2O monomer in acetonitrile (Figure 1b), we observe a pre-edge peak at 534.6 eV, a main-edge peak at 536.4 eV and a broad post-edge band 538.6 eV, similar to previous studies.[17] For this measurement with a molar fraction $x_{H_2O}=0.038$, hydrogen bonding is predominantly between water and acetonitrile, through two weak hydrogen bond interactions between H_2O and acetonitrile solvent molecules.[18] The spectral signatures of the H_2O monomer are therefore much akin to those of isolated H_2O molecules and we find in particular that the pre-edge peak also corresponds to the 1s core to the $4a_1$ LUMO transition. The broadening of the post-edge, covering the spectral region of transitions to Rydberg states in isolated H_2O molecules, indicates the impact of hydrogen bond donating interactions by H_2O to the acetonitrile solvent, with a smaller magnitude than those in bulk water.[18] In contrast to bulk water, an H_2O monomer in the aprotic solvent acetonitrile does not have hydrogen bond accepting interactions. It is because of the weak hydrogen bond donation, and the lack of hydrogen bond accepting interactions that the O K-edge XAS of H_2O monomer in acetonitrile reflect an electronic structure closer to that of gaseous H_2O, than that of bulk water.

For proton complexes prepared in a solution with 0.50 M HI/1.75 M H_2O in acetonitrile (stoichiometry $[H^+]:[H_2O]=1.0:3.5$), we observe a spectrum that is markedly distinct from the spectrum of the H_2O monomer in solution with a prominent absorption band centred at 539.6 eV and shoulders at 535.2, 537 and 542.0 eV (Figure 1c). As no significant absorption typical of water monomers occurs, in particular of the $1s\rightarrow 4a_1$ pre-edge peak at 534.6 eV, this result shows that at this solution composition, all water molecules are strongly associated with the proton as judged by the strength of the electronic interactions. This observation is in accordance with previous conclusions drawn from NMR and FT-IR measurements. Shoulders frequency up-shifted by 0.6 eV with respect to the monomer spectrum may indicate the positions of possible pre- and main-edge transitions of the hydrated proton complex with substantial decrease in relative absorption strength. Comparing H_2O monomer and the hydrated proton complex, the post-edge has a similar absorption strength. It is shifted by 1.0 eV to 539.6 eV with an additional contribution located near 542 eV. Based on these O K-edge XAS results we conclude that the electronic structure for all water molecules involved is significantly altered when a proton is hydrated by on average 3.5 water molecules. Because the spectral shape is so different from the H_2O monomer in solution beyond just spectral shifts of peaks, this experimental result directly shows that in hydrating the proton the largest fraction of, if not all, water molecules in the hydrated proton complex experience strong orbital mixing.

With the aim to reveal how this proton complex is further hydrated in acetonitrile solution, when the amount of water in the complex is increased, we compare in Figure 2a measurements with different stoichiometries ($[H^+]:[H_2O]=1.0:3.5$ and $1.0:8.0$). By adding 8 times more water than HI acid we observe marked increases in pre- and main-edges and a decrease in the post-edge. Moreover, the O K-edge spectrum still shows a shape clearly distinct from that of the water monomer with a pre-edge at 534.8 eV, a main-edge at 536.6 eV and a dominant post-edge with its maximum at 539 eV. This shows that from the perspective of oxygen K-edge XAS a full hydration of the proton in acetonitrile involves a large number of water molecules even with the higher water content.

To obtain further insight into how proton hydration affects the electronic structure of the water molecules involved, we have used the following approach: 1) determine with ab initio molecular dynamics (AIMD) simulations hydrogen bond strengths of hydrated proton complexes of different composition in acetonitrile and aqueous solution, both in nature of the hydrogen bond (superstrong, strong,

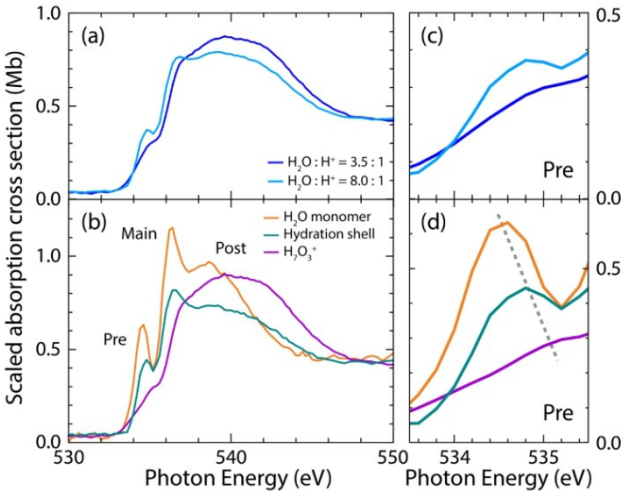

Figure 2. a) Measured O K-edge spectra scaled by oxygen number as measured for $[HI]:[H_2O]=1.0:3.5$ and $1.0:8.0$ (0.5 M HI:1.75 M H_2O and 0.5 M HI:4.0 M H_2O, respectively) in acetonitrile solution. b) Comparison of the spectral signatures of 0.75 M (orange) water in acetonitrile with those derived for the inner complex $H_7O_3^+$ (purple) and hydration shell water (dark cyan) around the inner complex $H_7O_3^+$ in acetonitrile. Panels (a), (b) show the excitation frequency range discussed in this study, and panels (c), (d) a blow-up of the pre-edge transition spectral region, to indicate the significant frequency shift of the pre-edge of hydration shell water around the inner hydrated proton complex compared to that of water in acetonitrile.

medium-strong and weak) and in possible distribution of hydrogen bond strengths due to interaction with the surrounding solvent; 2) estimate with quantum chemical calculations the impact of hydrogen bond interactions on the X-ray absorption bands of the individual water molecules that constitute the hydrated proton complexes; 3) derive from supporting FT-IR spectra possible complexation constants of hydrated proton complexes with which the stoichiometry and relative fractions of these complexes can be determined. These supporting FT-IR spectra have been recorded at 4 °C, to enable a better comparison to the oxygen K-edge measurements.

A direct insight into hydrogen bond strengths can be obtained by looking at the distances of the electronegative atoms that constitute the hydrogen bonds. O···O distance distribution functions $d(r)$ estimated from our AIMD simulations show (see Figure S4 and Table S1), that hydrated proton complexes in acetonitrile solution cover a broad range, from superstrong to weak hydrogen bonds, between the central H_3O^+ and the surrounding water molecules. Our results on $H_7O_3^+$ in acetonitrile are in close correspondence to earlier reported values obtained from QM/MM MD simulations.[11] Importantly, a clear hierarchy can be noted when comparing the close similarities of the O···O distance distribution functions $d(r)$ of $H_7O_3^+$ and of $H_{17}O_8^+$ in acetonitrile and of the hydrated proton in aqueous solution $H^+(aq)$ (see Figure S4, and Table S1), validating the generality of our model for how protons are hydrated. The architectural hierarchy, with concomitant magnitudes for orbital interaction strengths and hydrogen bond lengths, is thus similar for the hydrated proton complex in acetonitrile with a first hydration shell, and for the hydrated proton in bulk aqueous solution (cf. ref. [6b]). We find that the inner hydrated proton complex consists of a central H_3O^+ sharing the proton with a first water molecule w1 in a superstrong hydrogen bond (O···O distance 2.48 Å; such a short distance is characterized by a low barrier double well potential for the proton with distinct signatures in FT-IR[19] and 2D-IR spectra[5f,20a,b]). The central H_3O^+ forms a strong hydrogen bond with a second water molecule w2 (O···O distance 2.57 Å). It then takes at least another five additional water molecules to form a hydrated proton complex with a full first hydration shell around $H_7O_3^+$ to reach $H_{17}O_8^+$ in acetonitrile solution. Interestingly, a clearly weaker hydrogen bond between H_3O^+ and the third water molecule w3 occurs (O···O distance 2.68 Å), closer to the hydrogen bond lengths to first hydration shell water molecules around $H_7O_3^+$ (O···O distances range from 2.67–2.86 Å). From this important finding for hydrated proton complexes in liquid solution, be it in acetonitrile or in bulk solution, we can conclude that—in contrast to the gas phase case of $H_3O^+(H_2O)_3$ that is equivalent to the symmetric Eigen cation with equal hydrogen bond strengths between H_3O^+ and the three H_2O molecules—we can classify, from the hydrogen bond strength hierarchy perspective, w3 as rather being part of the first hydration shell water molecules than a constituent of the inner hydrated proton complex.

Three remarks on the findings of the structural hierarchy have to be made. Firstly, in the AIMD simulations all electronic degrees of freedom of the hydrated proton complexes and the surrounding solvent molecules have been treated quantum mechanically, whereas all nuclear degrees of freedom have been taken into account classically. Secondly, for the superstrong hydrogen bond the proton is shared between H_3O^+ and w1 in the so-called Zundel motif (i.e. $H_5O_2^+$), in such a fashion that it can only be properly taken into account using a full quantum treatment of the nuclear degrees of freedom of the shared proton,[5f] which would be numerically too costly to implement considering the sampling procedures that have to be used for oxygen K-edge XAS calculations. Thirdly, as the hydrogen bond length between H_3O^+ and w3 is much closer in value to those of w3 with its next hydration shell water molecules $w_{A,B}$ (and to those of w1, or w2 with their respective first hydration shell water molecules $w_{A,B}$ for that matter) than between H_3O^+ and w1 or w2, we argue that from a structural point of view the larger hydrated proton complexes in acetonitrile (and in aqueous solution) can be regarded as $H_7O_3^+$ with a surrounding hydration shell. From this it also follows that $H_9O_4^+$ should be better treated as $(H_7O_3^+)\cdot(H_2O)$, or alternatively as $[(H_5O_2^+)\cdot(H_2O)]\cdot(H_2O)$, and definitely not as the analogue of a symmetric Eigen cation in the gas phase. This structural hierarchy is not a static one: the roles of the individual water molecules in the hydrated proton complexes interchange upon ultrafast structural rearrangements of the water molecules forming the superstrong, strong, medium strong and weak hydrogen bonds, with ultrafast bond formation and cleavage dynamics of the hydrogen bonds with the hydration shell water molecules taking place on picosecond time scales.

Importantly, we now find that the hierarchy as found in hydrogen bond strengths and distances is also apparent in O K-edge XAS in the distinctly different spectral contributions of the 1s core excitations to the LUMOs of these water molecules hydrating the proton (see Figures S5 and S6). These spectra have been calculated using the half-core hole approximation[21] and for the hydrated proton complexes a classification has been defined based on the distance of the probed O atom in the complex from the central H_3O^+ (starting from H_3O^+ and identifying the first closest neighbour water molecule w1, to the next closest neighbour water molecule w2 etc.). A direct comparison of the calculated spectra, averaged over molecular configurations from our AIMD simulations, of H_3O^+, $H_5O_2^+$, $H_7O_3^+$ and $H_{17}O_8^+$ in acetonitrile with the calculated spectrum of the water monomer in acetonitrile solution shows that a direct relationship exists between average O···O distances and frequency upshifts and ratio of pre-edge/post-edge cross sections: the stronger the hydrogen bond the more upshifted the O K-edge and the more intense the post-edge is compared to that of the pre-edge. This result is much akin to that observed for the O K-edge spectra of water measured under different hydrogen bonding conditions,[13] yet—with now the hydrated proton in place—with markedly larger varying contributions in both spectral frequency shifts and relative absorption strengths of pre-edge and main-edge

bands the for hydrated proton complexes. This is in particular the case for the w1 and w2 molecules involved in a superstrong or strong hydrogen bond with the central H_3O^+. To determine how the XAS contributions of H_3O^+ and w1 change by having the proton fully shared between w0 and w1 in the low barrier superstrong hydrogen bond, we have investigated how the respective XAS contributions vary upon displacement of the proton along the superstrong O···H$^+$···O proton transfer coordinate (see Figure 3). As anticipated the XAS contributions become basically identical for both acetonitrile and aqueous solutions when the proton position is within 0.1 Å from the central position of the superstrong O···H$^+$···O proton transfer coordinate, with its relative magnitudes and spectral positions of pre-, main- and post-edge bands halfway between those of H_3O^+ and w1 (see Figure 3). Starting from w3 and the next hydration shell water molecules, the spectral contributions are similar in spectral position and shape. This is also apparent for the hydrated proton H^+(aq) in aqueous solution, underlying the large correspondence between proton hydration in acetonitrile and in aqueous solution.

We note that roles and interactions of the different water molecules in and around the hydrated proton complexes are

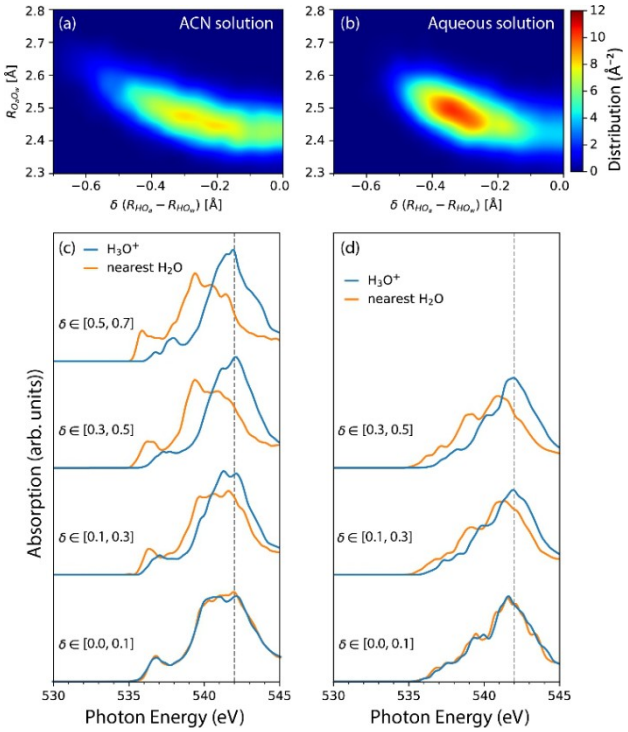

Figure 3. Structural correlations in the $H_5O_2^+$ (H_3O^+ and w1) species and associated sensitivity in the O K-edge XA spectra. Panels (a) and (b) display the correlation between the RO_a-O_b distance and the proton-asymmetry parameter "$\delta = RHO_a$-RHO_w" in the Zundel species for the simulations of $H_5O_2^+$ in acetonitrile solution and H^+(aq), respectively. Panels (c) and (d) contain the sampled O K-edge XA spectra for the central $H_5O_2^+$ (H_3O^+ and w1) species from simulations of $H_5O_2^+$ in acetonitrile solution and H^+(aq), respectively, decomposed into classes of varying O–H$^+$···O δ asymmetry from the symmetric species near δ ≈ 0 Å to highly asymmetric species with δ ≈ 0.5 Å.

subject to rapid solvent fluctuations and proton motions. We therefore use distance criteria to describe structural hierarchies of ensemble averages where each snapshot in the ensemble results from a particular ordering of the oxygen atoms. Importantly, we emphasize that the few femtosecond lifetimes and concomitant transverse dephasing times of 1s core excitations to the unoccupied molecular orbitals of the water molecules are orders of magnitude shorter than those of the solvent fluctuations associated with hydrogen bond rearrangements,[5d,h] electric field fluctuations imposed on the inner proton[5f,i,11] and von Grotthuss-type proton hopping between water molecules in the hydrated proton complexes.[1,6a,b–e,22] The x-ray snapshots that make up the measured x-ray absorption spectra are thus taken faster than solvent fluctuations and proton motions driven by these solvent fluctuations can affect the electronic transition coherences through spectral diffusion. Our experimental x-ray absorption results represent snapshots of a dynamically changing system that hydrated proton complexes are and can therefore be directly compared to ensemble averages from our calculations. It follows that the calculated O K-edge contributions of an individual water molecule in a hydrated proton complex will directly reflect the instantaneous hydrogen bond length distribution functions as estimated with the AIMD simulations. In addition, because the probe is local due to the localized O 1s core orbital, our probe provides information on the spatial extent over which the proton affects electronic structures.

FT-IR spectroscopy provides valuable information on the stoichiometries and hydrogen bonding characteristics of hydrated proton complexes in acetonitrile solution.[5b,f,i,11,20a,23] The hydrogen bonding hierarchy is evident from IR spectral marker bands. In particular the inner Zundel motif, $H_5O_2^+$ (i.e. w1···H$^+$···w0), has its inner proton transfer mode transition at 1250 cm^{-1}, its OH bending vibration located at 1725 cm^{-1} and its OH stretching mode band located in the spectral range of 2900–3400 cm^{-1}. These transitions are superimposed on a broad background known as the Zundel continuum that has its origin in the hyperpolarizability of the proton along the low barrier potential.[5f,i,9,11,19,20] The additional water molecules w2,..,w7 provide further contributions to the FT-IR spectrum with its OH bending and OH stretching bands centred at 1635 cm^{-1} and 3450–3480 cm^{-1}, respectively. While the OH bending transitions of these water molecules in the hydrated proton complexes are close to those of H_2O molecules themselves in acetonitrile solution (with a somewhat reduced oscillator strength[5i]), the markedly frequency downshifted OH stretching transitions observed for [HI]:[H_2O] ranging from 1:3.5 to 1:14 compared to the OH stretching band of H_2O in acetonitrile solution under similar concentration conditions provide conclusive evidence that the additional water molecules are essential parts of the larger hydrated proton complexes embedded in the acetonitrile solvent environment.

Based on the insights of the close correlation between hydrogen bond strengths/distances and O K-edge XAS features obtained from our AIMD simulations and the fact that a well-defined stoichiometry occurs for hydrated proton

complexes in acetonitrile (see FT-IR spectroscopic analysis in Supporting Information; Figures S7 and S8 and Table S2), we are now in the position to decompose our experimental O K-edge spectra of the $[H^+]:[H_2O]=1.0:3.5$ and $[H^+]:[H_2O]=1.0:8.0$ solutions in acetonitrile: We deduce spectra for the average inner $H_7O_3^+$ moiety (equivalent to a $[w1{\cdot}H_3O^+{\cdot}w2]/[H_5O_2^+{\cdot}w2]$ complex), and for the average first hydration shell water molecules around it (made up by w3 ··· w7, approximating that of $[\ H_7O_3^+{\cdot}(H_2O)_5\ ]$) (Figure 2b, see also Figure S3). We follow here the notion that the electronic structure of w3, the water molecule forming the third hydrogen bond with H_3O^+ has its characteristics inbetween that of w2 and to those of the next four hydration shell molecules w4···w7, but closer to that of w4 than that of w2. This means that from an electronic structure perspective, all three water molecules w1, w2 and w3 closest around H_3O^+, appear to follow the trend: the smaller the maximum value of the O···O distance distribution functions $d(r)$, the more frequency upshifted the respective calculated O K-edge XAS contributions. We compare these to the H_2O monomer in acetonitrile solution in Figure 2b. We conclude here that, in contrast to the symmetric Eigen complex $H_3O^+(H_2O)_3$ in the gas phase,[5e,24] solute-solvent interactions in acetonitrile and in aqueous solution make the hydrogen bond configuration around the central H_3O^+ to typically exhibit a large variation in hydrogen bond lengths/strengths. Our findings are fully consistent with calculated distance distribution functions reported before,[11] and also with FT-IR studies of hydrated proton complexes in acetonitrile,[5b] where the absence of the O–H stretching spectral signature of a symmetric Eigen complex $H_3O^+(H_2O)_3$ has been demonstrated.

We find that orbital interactions and hydrogen bonding in the inner $H_7O_3^+$ moiety are markedly different compared to those of its hydration-shell water and the water monomer. In addition to that, it is also clear that these interactions are different in the first hydration shell water molecules compared to those of H_2O monomer with significantly reduced pre- and main-edge intensities and a significantly shifted pre-edge peak. The spectral features of the hydration-shell water molecules appear to be intermediate between those of the inner $H_7O_3^+$ complex and those of the water monomer. The pre-edge peak energy in particular turns out to correlate with the degree of interactions with high energy for strong interactions and low energy for weak interactions (see Figure 2d, an effect clearly observable in the measured spectra in Figure 2c). We observe a substantial frequency up-shift of the pre-edge peak of 0.2 eV for the hydration shell water compared to the water monomer (along with an up-shift of 0.1 eV for the main-edge and diminished scaled cross sections of $\approx$30 % for both pre- and main-edges). These spectral differences and pre-edge peak shifts cannot be explained by increased water-water hydrogen-bonding interactions in the hydrated proton-complex sample alone as we estimate such interactions to result in a pre-edge up-shift of only 0.05 eV (see Figure S9).

To explain the measured spectral differences and the pre-edge peak shifts in Figure 2, we compare calculated spectra averaged over molecular configurations from our AIMD simulations of $H_7O_3^+$ and $H_{17}O_8^+$ in acetonitrile (as corresponding to concentrations of our two hydrated proton complex measurements) with the calculated spectrum of the water monomer in acetonitrile solution in Figure 4.

In good agreement with our $[H^+]:[H_2O]=1:3.5$ experiment (Figure 2a), the calculated spectra in Figure 4a of the different water molecules in $H_7O_3^+$ clearly show that the contributions of the central H_3O^+ and the two coordinated water molecules w1 and w2 exhibit a dominant peak at or above 540 eV (as the main- and post-edge contributions merge into one peak) and comparably weak pre-edge peaks, in marked difference to the water monomer spectrum. For H_3O^+ the main and post-edge peaks are caused by internal orbital hybridization within the H_3O^+ unit and by hybridization between H_3O^+ and the closest water molecules w1 and w2. The pre-edge in H_3O^+ is strongly reduced with respect to the water monomer by internal hybridization associated with changes in molecular symmetry. Going from C_{2v} in the monomer to C_{3v} in H_3O^+ reduces the amount of p-character of the LUMOs probed by O 1s core excitations[13b]). Going to the next layer of water molecules, the orbital interactions of w1 and w2 due to their superstrong and strong hydrogen bonds with the central H_3O^+ unit, respectively, causes the large differences of their spectra with respect to the water monomer. For a proper Zundel motif the hybridization of the two most inner water molecules sharing the proton in a superstrong hydrogen bond likely are identical, as calculations using a quantum treatment of the inner proton nuclear coordinate are expected to confirm. This directly supports our experimentally derived conclusion that all three water molecules in $H_7O_3^+$ experience strong orbital mixing. Because the spectral changes in the H_3O^+-w1-w2 sequence are largely retained for the $H_7O_3^+$ inner moiety in the $H_{17}O_8^+$ simulation as shown in Figure 4b, strong orbital mixing also dominates in the contribution of the $H_7O_3^+$ moiety in the experimental spectrum measured at increased water content (Figure 2b).

For the hydration shell water molecules w3 and beyond, the $H_{17}O_8^+$ simulation now enables us to explain and quantify the longer distance electronic structure effect of proton hydration beyond strong orbital mixing of those water molecules that are not in direct vicinity. Interestingly, the spectra of w3 and beyond are similar in shape to the monomer spectrum but pre- and main-edge intensities are not as large and the pre-edge peak is markedly shifted to higher energies.

Regarding, first, the spectral shape, we observe, both in experiment (Figure 2) and theory (Figure 4), that the further away a given water molecule is from the proton, the more closely its spectrum resembles that of the water monomer. Hydration shell water w3, w4, … obviously are hydrogen-bonded to the inner $H_7O_3^+$ moiety via their lone pairs and to the surrounding acetonitrile solvent through their respective O–H groups, but, given their spectral shape, the orbital interactions this entails are markedly weaker than those for w1 and w2. We note that the calculated spectra of w6 and w7 are nearly identical to that of the water monomer in acetonitrile because our $H_{17}O_8^+$ AIMD simulations fre-

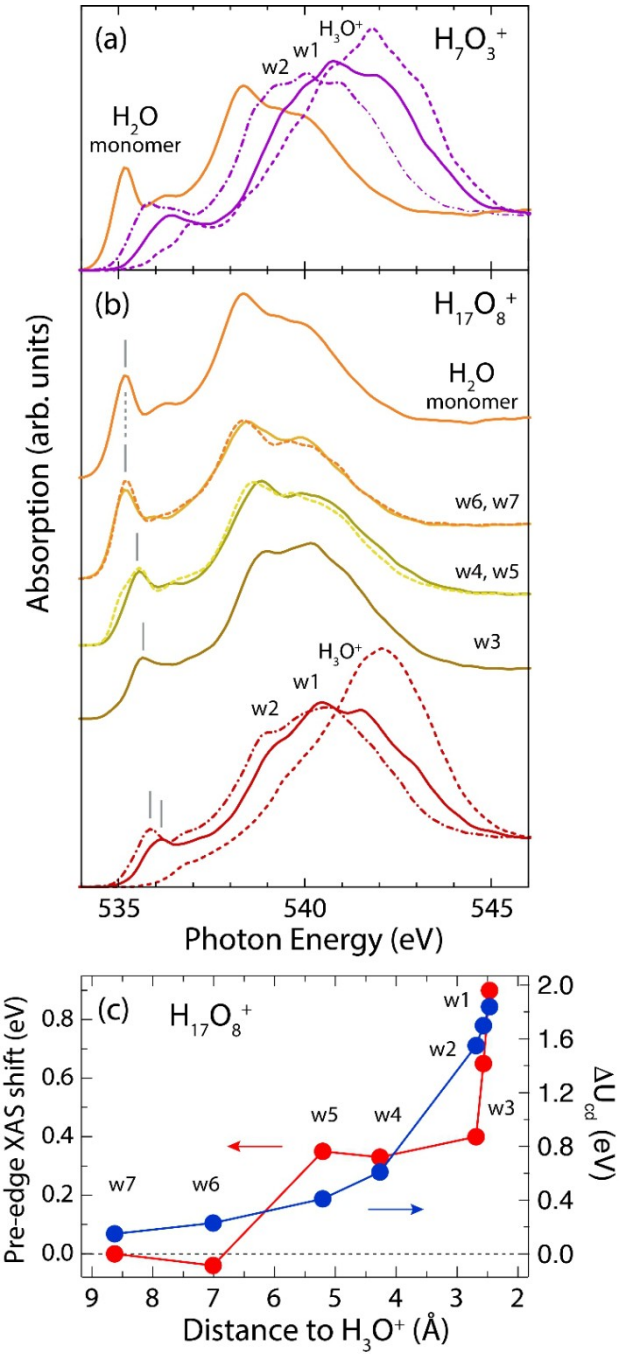

Figure 4. Theoretical O K-edge spectra sampled over AIMD simulations, calculated using the half-core hole approximation, decomposed by the respective contributions of the inner H_3O^+ (dashed lines), first closest neighbour H_2O (solid lines), second neighbour H_2O (dash-dotted lines) and water molecules at further distances (solid lines) for (a) H_2O monomer (orange) and $H_7O_3^+$ (purple), and (b) $H_{17}O_8^+$ (red, yellow and orange), all dissolved in acetonitrile. The magnitudes are scaled to each other. Panel (c) shows how for the individual water molecules of $H_{17}O_8^+$ in acetonitrile the change in dipole interaction energy ΔU_{cd} and the pre-edge frequency shift compares to the water monomer as a function of the distance from H_3O^+.

quently contains an intact $H_{13}O_6^+$ complex with w6 and w7 as two monomers with their lone pairs not involved in hydrogen bonding during the AIMD trajectories. From our analysis of the experimental FT-IR spectra (see Figure S8c and Table S2) we derive that intact hydrated proton complexes contain water molecules at least up to w6, for an average of 7.5 water molecules complexed with the proton for [HI]:[H_2O] = 1:8.

Regarding, second, the measured and calculated pre-edge peak energies, we find that the further away a water molecule is from the proton, the lower in energy the pre-edge peak is. The calculated pre-edge peak shifts of H_3O^+, w1, and w2 in $H_7O_3^+$ of 0.4–0.8 eV (with respect to the water monomer) and the measured shift of the experimental $H_7O_3^+$ spectrum of 0.6 eV (with respect to the monomer spectrum) agree well. Moreover, w4 and w5 in the $H_{17}O_8^+$ simulation correspond to the hydration-shell water contributions in experiment, and their calculated shifts of 0.3 eV and 0.2 eV with respect to the monomer, respectively, show satisfactory agreement with experiment (hydration shell spectrum with respect to monomer). These observations motivate plotting in Figure 4c the calculated pre-edge shift for the various water molecules of our $H_{17}O_8^+$ AIMD simulation as a function of distance to the central H_3O^+ unit. We find a clear trend that suggests that the magnitude of the average pre-edge frequency shift for a given class of water molecule w1, w2, … in the hydrated proton complex directly depends on the proximity of that class of water molecule to the central H_3O^+ unit. At short distances the spectrum is dominated by spectral changes due to orbital interactions, whereas at larger distances the spectral shape is constant but the trend of the pre-edge peak shift with distance to the proton appears to prevail. Because for distant molecules the influence of orbital interactions on the spectrum is strongly decreased, the pre-edge peak frequency position indicates a correlation due to an additional electronic structure effect caused by the proton.

The pre-edge band is due to transitions of the oxygen 1s core level to the strongly oriented and far-out reaching $4a_1$ orbital (see also Figure 1d,e,f). Our calculated spectra indicate that the energy of this orbital as we probe it with XAS shifts to higher energies the closer the given water molecule is to the proton. We find that, the more a given class of molecules is exposed to the electro-static field of the proton, the larger this shift is. To confirm this observation we evaluated the change in dipole energy ΔU_{cd} due to pre-edge excitation in a water monomer (isolated gas-phase-like). We placed this monomer in the electric field of a proton charge and calculated ΔU_{cd} for varied distances to the proton. We thus use this monomer as a test dipole to estimate the effect of the proton electric field onto the pre-edge orbital energy. We now plot the calculated values of ΔU_{cd} as a function of distance to the proton for those water molecules belonging to the different classes w1, w2, …, in our $H_{17}O_8^+$ simulation in Figure 4c (ΔU_{cd} is set to zero for the isolated case; "distance to the proton" and "distance to H_3O^+" are used synonymously for simplicity). Apparently, this simple model qualitatively reproduces the trend of the calculated pre-edge shifts of w1, w2, etc. and the resulting correlation lets us conclude that the observed pre-edge shift is a measure of the electric field strength of the proton (with

estimated values varying between 10 to more than 200 MV cm^{-1}, see Figure S10 for electric field strengths as a function to distance to the proton). The fields imposed by the dipoles of the surrounding acetonitrile solvent molecules amount to 20–30 MV cm^{-1}.[11] The electrical fields due to the positive charge of the proton clearly exceed the solvent-induced fields by a factor of 2 for the hydration shell water molecules to 7 for the two water molecules bound to H_3O^+ in the $H_7O_3^+$ inner proton complex). With this finding we conclude that the impact of the proton in modifying the electronic structure of water extends to at least one hydration shell around the $H_7O_3^+$ inner moiety. While the hydration-shell water molecules are not significantly altered by orbital interactions, they are mostly affected by the Coulomb potential and the associated electric field of the proton via a shift of their LUMO-4a$_1$ orbital energy. The gradual transition we find for hydrated proton complexes from dominant orbital interactions in defined molecular geometries close to the proton to orbital energy shifts due to the electric field of the proton at larger distances will influence the way we quantify and control the interactions of water molecules with protons in nature, ultrafast proton transfer reactions in solution and in technological devices based on proton transfer processes.

Conclusion

We have shown how, layer by layer, with soft x-ray spectroscopy we can reveal to what extent the orbitals of water molecules are affected by hydrating a proton. In a combined experimental and theoretical study we find orbital-specific markers that distinguish two main electronic-structure effects: Local orbital interactions determine covalent bonding between the proton and neigbouring water molecules, while orbital-energy shifts measure the strength of the extended electric field of the proton. The ensemble average provided by the oxygen K-edge spectroscopic snapshots, as measured by the local core-excitations, provides a direct insight into proton hydration beyond the conventional Eigen and Zundel pictures of particular geometries, $H_3O^+(H_2O)_3$ and $H_5O_2^+$, respectively. Our study provides a new approach highlighting a gradual transition from strong orbital interactions of the hydrated proton with proximal water molecules to orbital-energy shifts induced in distal water molecules, that will be of much use in steady-state investigations of hydrated protons and time-resolved studies of the underlying mechanisms of aqueous proton transport.

Acknowledgements

We cordially acknowledge support by Stephan Figul (Advanced Microfluidic Systems GmbH) in the implementation and temperature calibration of the acetonitrile flatjet system. Funding: M. Ekimova, C. Kleine, J. Ludwig and E.T.J. Nibbering acknowledge support from the German Science Foundation (Project Nr. DFG—NI 492/11-1) and the European Research Council (ERC) under the European Union's Horizon 2020 research and innovation programme (ERC Grant Agreement N° 788704; E.T.J.N.). M. Odelius acknowledges support from the Carl Tryggers Foundation (contract CTS18:285) and the European Union's Horizon 2020 research and innovation programme under the Marie Skłodowska-Curie grant agreement No 860553. The calculations were enabled by resources provided by the Swedish National Infrastructure for Computing (SNIC) partially funded by the Swedish Research Council through grant agreement no. 2018–05973. N. Huse gratefully acknowledges funding by the Cluster of Excellence 'CUI: Advanced Imaging of Matter' of the Deutsche Forschungsgemeinschaft – EXC2056 – projectID390715994. E. Pines acknowledges support from the Israel Science Foundation (grant number 1587/16). We all greatly acknowledge the support of the BESSYII staff during x-ray measurements at the UE52_SGM Undulator SGM variable polarisation beamline of the Helmholtz-Zentrum Berlin and we thank Helmholtz-Zentrum Berlin for the allocation of synchrotron radiation beamtime. Authors contributions: M.E. and E.T.J.N. started and planned the project, with early add-ons by Ph.W. and M.Od.; M.E., C.K., J.L. and M.Oc. performed the XAS experiments; M.E. and C.K. analysed the XAS experimental data; E.K., D.P and E.P. performed and analysed the FT-IR experiments; T.E.G.A. and M.Od. performed and analysed the AIMD simulations; E.T.J.N. wrote the manuscript with contributions from M.E., C.K., E.P., Ph.W. and M.Od. and further amendments by J.L., M.Oc., T.E.G.A. and N.H.. Open Access funding enabled and organized by Projekt DEAL.

Conflict of Interest

The authors declare no conflict of interest.

Data Availability Statement

The data that support the findings of this study are available from the corresponding author upon reasonable request.

Keywords: Eigen Cation · Electronic Structure · Hydrated Proton · Soft X-Ray Absorption Spectroscopy · Zundel Cation

[1] D. Marx, M. E. Tuckerman, J. Hutter, M. Parrinello, *Nature* **1999**, *397*, 601–604.
[2] M. Eigen, *Angew. Chem. Int. Ed. Engl.* **1964**, *3*, 1–19; *Angew. Chem.* **1963**, *75*, 489–508.
[3] a) M. A. Hickner, H. Ghassemi, Y. S. Kim, B. R. Einsla, J. E. McGrath, *Chem. Rev.* **2004**, *104*, 4587–4611; b) K.-D. Kreuer, S. J. Paddison, E. Spohr, M. Schuster, *Chem. Rev.* **2004**, *104*, 4637–4678.
[4] T. E. DeCoursey, *Physiol. Rev.* **2013**, *93*, 599–652.
[5] a) O. F. Mohammed, D. Pines, J. Dreyer, E. Pines, E. T. J. Nibbering, *Science* **2005**, *310*, 83–86; b) N. Ben-Menachem Kalish, E. Shandalov, V. Kharlanov, D. Pines, E. Pines, *J. Phys. Chem. A* **2011**, *115*, 4063–4075; c) E. Freier, S. Wolf, K. Gerwert, *Proc. Natl. Acad. Sci. USA* **2011**, *108*, 11435–11439;

d) M. Thämer, L. De Marco, K. Ramasesha, A. Mandal, A. Tokmakoff, *Science* **2015**, *350*, 78–82; e) C. T. Wolke, J. A. Fournier, L. C. Dzugan, M. R. Fagiani, T. T. Odbadrakh, H. Knorke, K. D. Jordan, A. B. McCoy, K. R. Asmis, M. A. Johnson, *Science* **2016**, *354*, 1131–1135; f) F. Dahms, B. P. Fingerhut, E. T. J. Nibbering, E. Pines, T. Elsaesser, *Science* **2017**, *357*, 491–494; g) V. A. Lorenz-Fonfria, M. Saita, T. Lazarova, R. Schlesinger, J. Heberle, *Proc. Natl. Acad. Sci. USA* **2017**, *114*, E10909–E10918; h) J. A. Fournier, W. B. Carpenter, N. H. C. Lewis, A. Tokmakoff, *Nat. Chem.* **2018**, *10*, 932–937; i) E. Kozari, M. V. Sigalov, D. Pines, B. P. Fingerhut, E. Pines, *ChemPhysChem* **2021**, *22*, 716–725.

[6] a) K. Ando, J. T. Hynes, *J. Phys. Chem. B* **1997**, *101*, 10464–10478; b) O. Markovitch, H. Chen, S. Izvekov, F. Paesani, G. A. Voth, N. Agmon, *J. Phys. Chem. B* **2008**, *112*, 9456–9466; c) J. Xu, Y. Zhang, G. A. Voth, *J. Phys. Chem. Lett.* **2011**, *2*, 81–86; d) W. Kulig, N. Agmon, *Nat. Chem.* **2013**, *5*, 29–35; e) A. Hassanali, F. Giberti, J. Cuny, T. D. Kühne, M. Parrinello, *Proc. Natl. Acad. Sci. USA* **2013**, *110*, 13723–13728.

[7] E. Wicke, M. Eigen, T. Ackermann, *Z. Phys. Chem.* **1954**, *1*, 340–364.

[8] J.-O. Lundgren, I. Olovsson in *The hydrogen bond: Recent developments in theory and experiments, Vol. II* (Eds.: P. Schuster, G. Zundel, C. Sandorfy), North Holland, Amsterdam, **1976**, pp. 471–526.

[9] G. Zundel, H. Metzger, *Z. Phys. Chem. Neue Folge* **1968**, *58*, 225–245.

[10] H.-H. Limbach, P. M. Tolstoy, N. Pérez-Hernández, J. Guo, I. G. Shenderovich, G. S. Denisov, *Isr. J. Chem.* **2009**, *49*, 199–216.

[11] A. Kundu, F. Dahms, B. P. Fingerhut, E. T. J. Nibbering, E. Pines, T. Elsaesser, *J. Phys. Chem. Lett.* **2019**, *10*, 2287–2294.

[12] J. W. Smith, R. J. Saykally, *Chem. Rev.* **2017**, *117*, 13909–13934.

[13] a) P. Wernet, D. Nordlund, U. Bergmann, M. Cavalleri, M. Odelius, H. Ogasawara, L. Å. Näslund, T. K. Hirsch, L. Ojamäe, P. Glatzel, L. G. M. Pettersson, A. Nilsson, *Science* **2004**, *304*, 995–999; b) A. Nilsson, D. Nordlund, I. Waluyo, N. Huang, H. Ogasawara, S. Kaya, U. Bergmann, L.-Å. Näslund, H. Öström, P. Wernet, K. J. Andersson, T. Schiros, L. G. M. Pettersson, *J. Electron Spectrosc. Relat. Phenom.* **2010**, *177*, 99–129.

[14] a) M. Ekimova, W. Quevedo, Ł. Szyc, M. Iannuzzi, P. Wernet, M. Odelius, E. T. J. Nibbering, *J. Am. Chem. Soc.* **2017**, *139*, 12773–12783; b) Z.-H. Loh, G. Doumy, C. Arnold, L. Kjellsson, S. H. Southworth, A. Al Haddad, Y. Kumagai, M.-F. Tu, P. J. Ho, A. M. March, R. D. Schaller, M. S. B. Yusof, T. Debnath, M. Simon, R. Welsch, L. Inhester, K. Khalili, K. Nanda, A. I. Krylov, S. Moeller, G. Coslovich, J. Koralek, M. P. Minitti, W. F. Schlotter, J.-E. Rubensson, R. Santra, L. Young, *Science* **2020**, *367*, 179–182.

[15] a) C. D. Cappa, J. D. Smith, B. M. Messer, R. C. Cohen, R. J. Saykally, *J. Phys. Chem. B* **2006**, *110*, 1166–1171; b) M. Cavalleri, L. A. Näslund, D. C. Edwards, P. Wernet, H. Ogasawara, S. Myneni, L. Ojamäe, M. Odelius, A. Nilsson, L. G. M. Pettersson, *J. Chem. Phys.* **2006**, *124*, 194508.

[16] J. Stöhr, *NEXAFS Spectroscopy, Vol. 25*, Springer, Berlin, **1996**.

[17] M. Nagasaka, H. Yuzawa, N. Kosugi, *J. Phys. Chem. B* **2020**, *124*, 1259–1265.

[18] a) Y. Marcus, Y. Migron, *J. Phys. Chem.* **1991**, *95*, 400–406; b) J. E. Bertie, Z. D. Lan, *J. Phys. Chem. B* **1997**, *101*, 4111–4119.

[19] G. Zundel, *Adv. Chem. Phys.* **2000**, *111*, 1–217.

[20] a) F. Dahms, R. Costard, E. Pines, B. P. Fingerhut, E. T. J. Nibbering, T. Elsaesser, *Angew. Chem. Int. Ed.* **2016**, *55*, 10600–10605; *Angew. Chem.* **2016**, *128*, 10758–10763; b) B. Dereka, Q. Yu, N. H. C. Lewis, W. B. Carpenter, J. M. Bowman, A. Tokmakoff, *Science* **2021**, *371*, 160–164.

[21] a) L. Triguero, L. G. M. Pettersson, H. Ågren, *Phys. Rev. B* **1998**, *58*, 8097–8110; b) M. Iannuzzi, J. Hutter, *Phys. Chem. Chem. Phys.* **2007**, *9*, 1599–1610.

[22] S. Meiboom, *J. Chem. Phys.* **1961**, *34*, 375–388.

[23] M. V. Sigalov, N. Kalish, B. Carmeli, D. Pines, E. Pines, *Z. Phys. Chem.* **2013**, *227*, 983–1007.

[24] J. M. Headrick, E. G. Diken, R. S. Walters, N. I. Hammer, R. A. Christie, J. Cui, E. M. Myshakin, M. A. Duncan, M. A. Johnson, K. D. Jordan, *Science* **2005**, *308*, 1765–1769.

Manuscript received: July 27, 2022
Accepted manuscript online: September 14, 2022
Version of record online: October 25, 2022